MINISTRY OF EDUCATION AND TRAINING

VIETNAM ACADEMY OF SCIENCE AND TECHNOLOGY

GRADUATE UNIVERSITY SCIENCE AND TECHNOLOGY

Pham Thi Tot

Study on fabrication of photoelectrochemical composite electrode of PbO_2, TiO_2 and SnO_2 to treat Methyl Orange

Major: Theoretical and Physical Chemistry

Code: 9440119

SUMMARY OF CHEMISTRY DOCTORAL THESIS

Ha Noi - 2023

The thesis was completed at: Graduate University Science and Technology - Vietnam Academy of Science and Technology

Instructor 1: Assoc. Prof. Dr. Phan Thi Binh
Instructor 1: Dr. Mai Thi Thanh Thuy

Reviewer 1:
Reviewer 2:
Reviewer 3:

The thesis was defended at the doctoral thesis review committee, meeting in Graduate University of Science and Technology, Vietnam Academy of Science and Technology from…. .. to …., date, month, 2023

The thesis can be found in:
- Library of Graduate University of Science and Technology
- National Library of Vietnam

INTRODUCTION

1. The necessary of thesis

Along with the development of economy and industry, the problem of environmental pollution is increasingly serious, including water pollution. One of the most common types of pollutants is dyes. Dyes have entered the water resources from different industries such as textile, food, paper and printing. The wastewater seriously affects the environment and human health. The wastewater of the industries cause serious environmental pollution and affect human health. If the content of dyes in water is high, it will affect the growth and development of aquatic species because the ability to regenerate oxygen and absorb sunlight is reduced. Currently, the dye industry is also very developed with many dyes, so the dyeing wastewater sources also have very different characteristics. Among the dyes, methyl orange (MO) is also interested by many scientists because it is toxic to environment and human health. MO is difficult to remove due to high water solubility and low biodegradability. Currently, there are many methods to removal dyes in wastewater such as adsorption, coagulation–,flocculation, biological treatment, and electrocatalytic oxidation. The electrocatalytic oxidation method has many significant advantages such as easy operation, laboratory temperature and pressure, high degradation efficiency, and no secondary pollution generation. For these catalytic processes, the anode material is very important because it will directly affect the efficiency of organic removal. The requirements of anode material are inert, dimensionally stable, good conductive, have the ability to catalyze electrochemical for reactions and high oxygen over potential.

Lead dioxide (PbO_2) is a stable structure material, good conductive, and high oxygen over potential. Therefore, PbO_2 is often used in many fields such as electrochemical sensors, anode material to catalyze electrochemical reactions, anode material for battery, anode material to treat wastewater of paper industry,... In order to improve the electrochemical catalytic ability and increase the durability of materials, PbO_2 hybrid with metal oxides to create composite materials. In this thesis, PbO_2 is modified with TiO_2 and SnO_2 to create composites PbO_2-TiO_2, PbO_2-SnO_2, and PbO_2-TiO_2-SnO_2 used as anode materials for the treatment of MO.

2. The aims of thesis

- Determine optimal conditions to synthesis of PbO_2 and modified PbO_2 with TiO_2; SnO_2 to create PbO_2-TiO_2; PbO_2-SnO_2 and PbO_2-TiO_2-SnO_2 composites on stainless steel (SS) substrate;

- Study on the morphological structure, electrochemical and photoelectrochemical properties of PbO_2, composites of PbO_2 with TiO_2 and SnO_2;

- Using PbO_2 and composites of PbO_2 with TiO_2; SnO_2 as the anode for MO treatment by electrochemical and photoelectrochemical methods.

3. The main contents of thesis

- Research on synthesizing PbO_2 on SS substrate by cyclic voltammetry (CV) method (changing the number of cycles and scan rate);

- Research on modification of PbO_2 with TiO_2; SnO_2 to create PbO_2-TiO_2; PbO_2-SnO_2, and PbO_2-TiO_2-SnO_2 composites on SS substrate;

- Study on morphological structure, electrochemical and photoelectrochemical properties of PbO_2 and its composites with TiO_2 and SnO_2;

- Research on MO treatment by electrochemical and photoelectrochemical methods using PbO_2 and its composites with TiO_2; SnO_2 anode electrode;

- Study on the kinetic of MO processing and oxidation - reduction potential (ORP) of the solution before and after treatment. Proposed treatment mechanism.

CHAPTER 1. OVERVIEW

The overview sections collect and analyze domestic and foreign issues related to the thesis's content.

1.1. Selection basis anode electrode material for electrochemical and photoelectrochemical catalyst oxidation processes

1.2. Introduction to lead dioxide, titanium dioxide, tin dioxide

1.3. Composite based on PbO_2 with TiO_2 and SnO_2

1.4. Wastewater

CHAPTER 2. EXPERIMENT AND METHOD

2.1. Experimental

Using IM6 device to synthesize PbO_2 and composite materials based on PbO_2, TiO_2, SnO_2 on SS subtrate by CV method. The schematic diagram of the synthesis process is shown in Figure 2.1.

MO is treated by constant current method on IM6 device using 3 electrode system: counter electrode (Pt plate), reference electrode (Ag/AgCl, saturated KCl), and working electrode (SS/PbO_2, SS/PbO_2-TiO_2, SS/PbO_2-SnO_2, SS/PbO_2-TiO_2-SnO_2). The schematic diagram of the MO treatment process is shown in Figure 2.2.

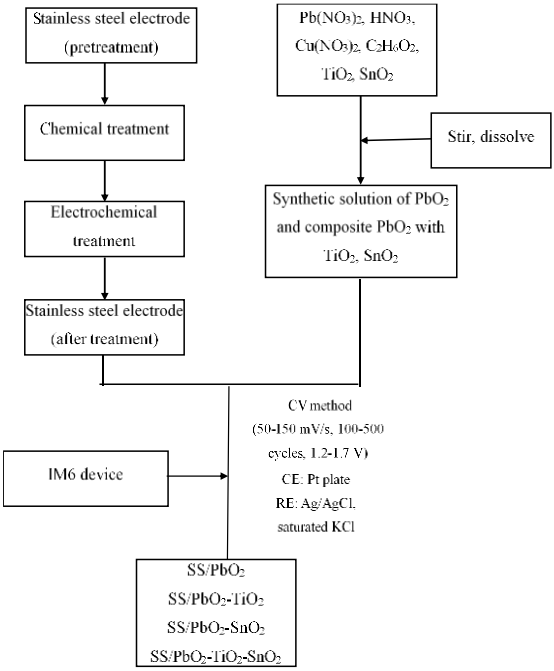

Figure 2.1. The schematic diagram of the synthesis process PbO_2 and composite of PbO_2, TiO_2, SnO_2

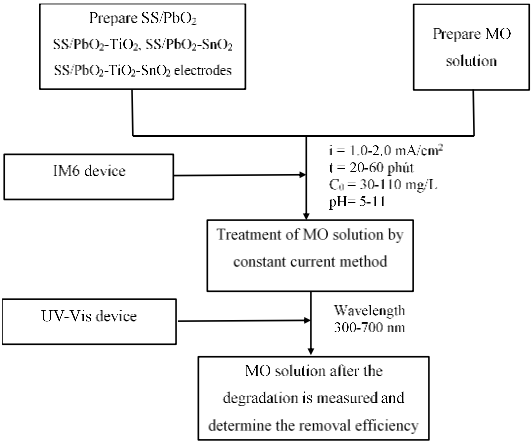

Figure 2.2. The schematic diagram of the MO treatment

2.2. Research methods

- Cyclic voltammetry method
- Electrochemical Impedance Spectroscopy method

- Potentiodynamic polarization method
- Constant current method
- Energy Dispersive X-ray, Scanning Electron Microscope and measuring electrode material layer thickness mehtod
- Ultraviolet-Visible method
- High Performance Liquid chromatography–mass spectrometry method
- Oxidation - reduction potential measuring method
- pH measuring method
- Brunauer – Emmet – Teller measuring method
- The adhesion of electrode materials measuring method

CHAPTER 3. RESULTS AND DISCUSSION

3.1. Research on material synthesis conditions

3.1.1. Mechanism of PbO_2 formation on stainless steel substrate

PbO_2 was synthesized directly on SS by CV method from a mixed solution 0.5 M $Pb(NO_3)_2$; 0.1 M HNO_3; 0.05 M $Cu(NO_3)_2$, and 0.1 M $C_2H_6O_2$. The mechanism of PbO_2 formation on SS substrate is according to equations (1.6)-(1.8) (see section 1.2). PbO_2 synthesis efficiency is quite high, reaching from 96.48-99.25%.

$$OH^- \rightarrow OH_{ads} + e^- \quad (1.6)$$

$$Pb^{2+} + OH_{ads} + OH^- \rightarrow Pb(OH)_2^{2+} + e^- \quad (1.7)$$

$$Pb(OH)_2^{2+} \rightarrow PbO_2 + 2H^+ \quad (1.8)$$

3.1.2. Effect of CV number during synthesis on the electrochemical properties of the SS/PbO_2 electrode

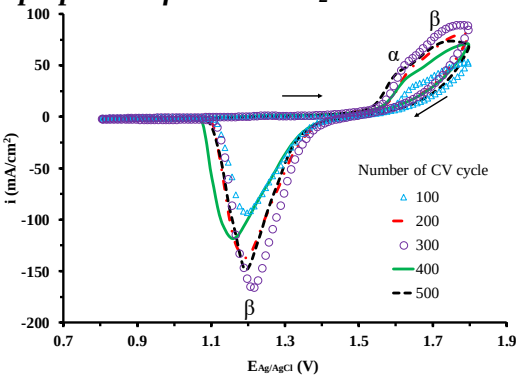

Figure 3.3. Effect of the number of CV (systhesis condition: scan rate 50 mV/s, potential range 1.2-1.7 V) on cyclic voltammograms of SS/PbO_2 electrode in 0.5 M H_2SO_4 (the 30th cycle, scan rate 100 mV/s, potential range 0.8 -1.8 V)

Table 3.4. Effect of CV number (scan rate 50 mV/s) on the electrochemical parameters is determined from Figure 3.4.

Number of CV (cycle)	i_o ($\mu A/cm^2$)	E_o (V)
100	22.22	1.245
200	39.63	1.256
300	61.93	1.265
400	55.17	1.257
500	42.35	1.249

When the SS/PbO_2 electrode was fabricated with 300 cycles, its redox peak reached the highest value and exchange current density was the highest (61.93 mA/cm^2), indicating the best electrocatalytic ability.

3.1.3. Effect of scanning speed during synthesis on electrochemical properties of SS/PbO_2 electrode

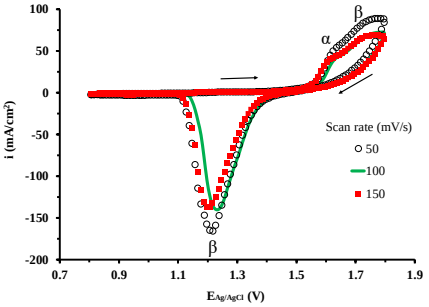

Figure 3.5. Effect of scanning speed (systhesis condition: 300 cycles, potential range 1.2-1.7 V) on cyclic voltammograms of SS/PbO_2 electrode in 0.5 M H_2SO_4 (the 30th cycle, scan rate 100 mV/s, potential range 0.8 -1.8 V)

Table 3.6. Effect of scanning speed (300 cycles) on the electrochemical parameters is determined from Figure 3.6

Scanning speed (mV/s)	i_o (μA/cm^2)	E_o (V)
30	57.32	1.236
50	61.93	1.265
100	24.03	1.237
150	21.55	1.267

When the SS/PbO_2 electrode was synthesized at 50 mV/s, its redox peak reached the highest value and exchange current density was the biggest (61.93 mA/cm^2), indicating the best electrocatalytic ability.

3.1.4. Effects of TiO_2 and SnO_2 concentrations in the synthesis of composite

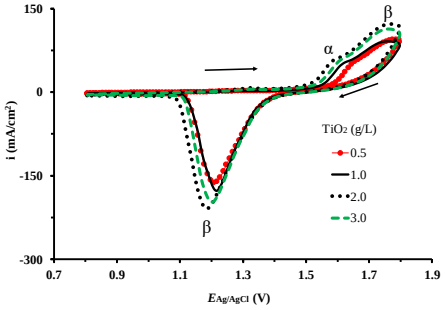

Figure 3.7. Effects of TiO_2 concentration on cyclic voltammograms of SS/PbO_2-TiO_2 composite electrode in 0.5 M H_2SO_4 (the 30th cycle, scan rate 100 mV/s, potential range 0.8 -1.8 V)

Table 3.8. Effects of TiO_2 concentration (sythesis condition: 300 cycles, 50 mV/s) on the electrochemical parameters is determined from Figure 3.8

TiO_2 concentration (g/L)	i_o (μA/cm^2)	E_o (V)
0.5	39.63	1.263
1.0	44.23	1.243
2.0	53.43	1.254
3.0	56.62	1.225

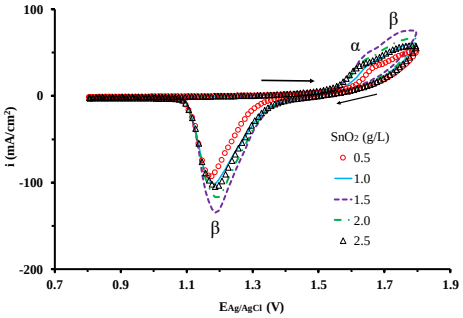

Figure 3.9. Effects of TiO_2 concentration on cyclic voltammograms of SS/PbO_2-SnO_2 composite electrode in 0.5 M H_2SO_4 (the 30th cycle, scan rate 100 mV/s, potential range 0.8 -1.8 V)

Table 3.10. Effects of SnO_2 concentration (sythesis condition: 300 cycles, 50 mV/s) on the electrochemical parameters is determined from Figure 3.10

SnO_2 concentration (g/L)	i_o ($\mu A/cm^2$)	E_o (V)
0.5	60.51	1.249
1.0	64.05	1.262
1.5	65.12	1.251
2.0	63.69	1.249
2.5	59.45	1.262

The results showed that SS/PbO_2-TiO_2 and SS/PbO_2-SnO_2 electrodes with 2.0 g/L TiO_2 and 1.5 g/L SnO_2 have the best electrochemical activity (Figure 3.7 and Table 3.8; Figure 3.9 and Table 3.10, respectively). When both TiO_2 (2.0 g/L) and SnO_2 (1.5 g/L) used concurrently during synthesis, the obtained SS/PbO_2-TiO_2-SnO_2 composite electrode has the best activity (Figure 3.11, Table 3.12).

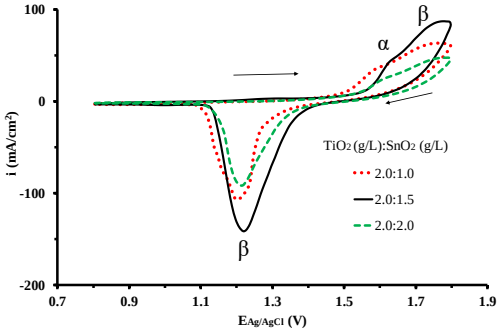

Figure 3.11. Effects of TiO_2 and SnO_2 concentration on cyclic voltammograms of SS/PbO_2-TiO_2-SnO_2 composite electrode in 0.5 M H_2SO_4 (the 30th cycle, scan rate 100 mV/s, potential range 0.8 -1.8 V)

Table 3.12. Effects of TiO_2:SnO_2 concentration (sythesis condition: 300 cycles, 50 mV/s) on the electrochemical parameters is determined from Figure 3.12

TiO_2:SnO_2 (g/L)	i_o ($\mu A/cm^2$)	E_o (V)
2.0:1.0	89.17	1.214
2.0:1.5	101.90	1.220
2.0:2.0	79.62	1.188

3.2. Study on the morphological structure of PbO_2 and PbO_2 with TiO_2; SnO_2 composites

3.2.1. X-ray diffraction

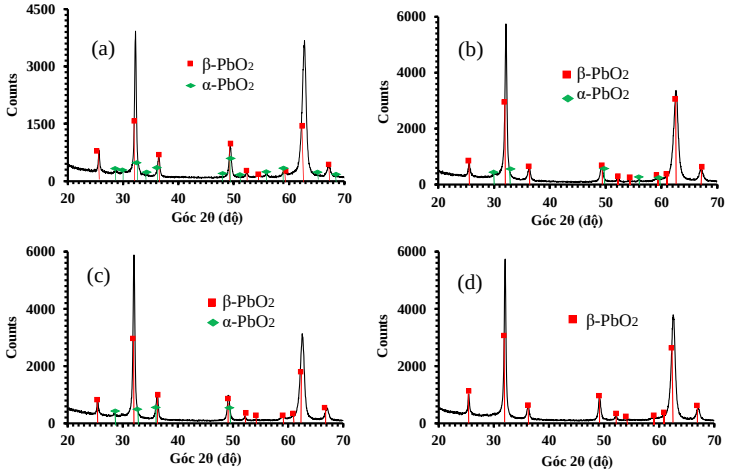

Figure 3.13. XRD spectrum (a) PbO_2, (b) PbO_2-TiO_2 composite (c) PbO_2-SnO_2 composite, (d) PbO_2-TiO_2-SnO_2 composite

The appearance of typical peaks for β-PbO_2 and α-PbO_2 form (Figure 3.13) proves that PbO_2 material has been successfully synthesized in both crystalline forms. However, the peaks of TiO_2 and SnO_2 do not appear due to their very small size and low amount, so it is difficult to emit reflected rays when X-rays are shined.

3.2.2. EDX spectrum

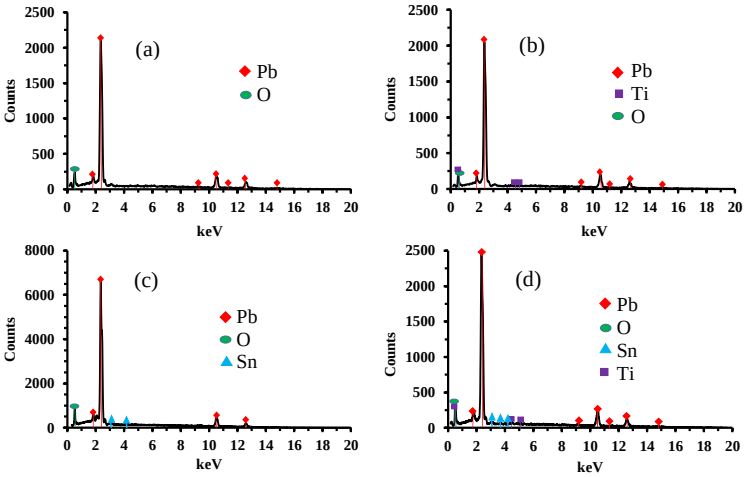

Figure 3.14. EDX spectrum (a) PbO_2, (b) PbO_2-TiO_2 composite (c) PbO_2-SnO_2 composite, (d) PbO_2-TiO_2-SnO_2 composite

From the EDX spectrum (Figure 3.14), it is clear that the typical peaks for Pb, O, Ti, Sn. This proves the presence of TiO_2 and SnO_2 in the composite. Thus, it can be said that composites have been successfully synthesized on the basis of PbO_2, TiO_2 and SnO_2 by CV method.

3.2.3. Element-Mapping spetrum

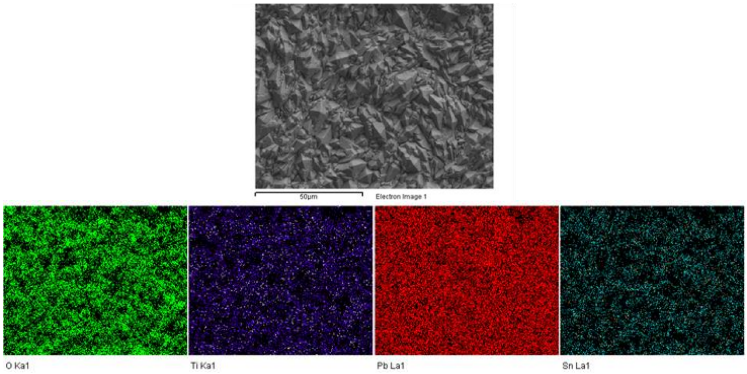

Figure 3.15. Element-mapping spectrum of SS/PbO_2-TiO_2-SnO_2 composite electrode (sythesis condition: 300 cycles, 50 mV/s)

The Element-mapping spectrum of PbO_2-TiO_2-SnO_2 composite is shown the green, purple, red and blue colours representing the presence of elements O, Ti, Pb and Sn in the composite, respectively.

3.2.4. SEM observation

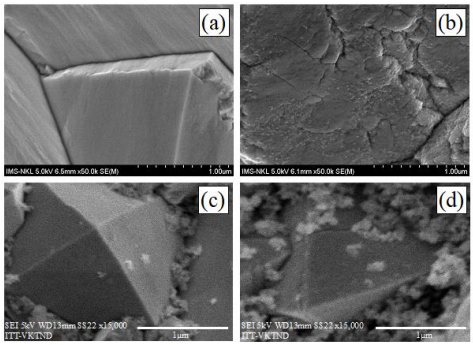

Figure 3.16. SEM image (a) PbO_2, (b) PbO_2-TiO_2 composite (c) PbO_2-SnO_2 composite, (d) PbO_2-TiO_2-SnO_2 composite

SEM image of PbO_2 (Figure 3.16a) shows large tetrahedral crystals interspersed with small crystals. The large crystals are the structure of β-PbO_2 while the small crystals belong to the structure of α-PbO_2, indicating that the

material contains both forms. On the composites, TiO_2 and SnO_2 crystals were located on the surface and interspersed between the PbO_2 crystals (Fig. 3.16b-d).

3.2.5. Adsorption isotherm

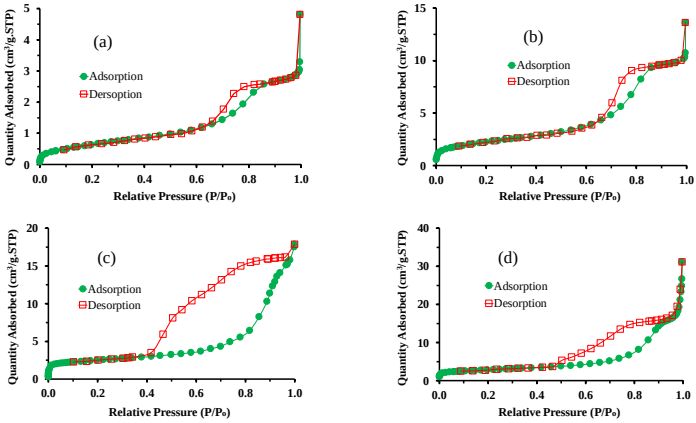

Figure 3.17. Adsorption isotherm (a) PbO_2, (b) PbO_2-TiO_2 composite (c) PbO_2-SnO_2 composite, (d) PbO_2-TiO_2-SnO_2 composite

The adsorption isotherm (Figure 3.17) of the PbO_2 and the composites are type IV with a hysteresis loop between the adsorption and desorption curves. The PbO_2-TiO_2-SnO_2 composite has a larger specific surface area than that of PbO_2 and two- composites (PbO_2-TiO_2; PbO_2-SnO_2). Because TiO_2 and SnO_2 doped into composites the number of solid particles increased on their surface, moreover, nano-sized TiO_2 and SnO_2 particles also contribute to the increase of the specific surface area of the composite.

3.2.6. Determine the thickness of the electrode material layer

Table 3.15. The thickness of the electrode material layer on SS substrate

Measurement position	The thickness of the material layer (μm)			
	PbO_2	PbO_2-TiO_2	PbO_2-SnO_2	PbO_2-TiO_2-SnO_2
The first position	247,0	305,002	374,005	420,005
The second position	239,033	303,015	344,006	428,042
The third position	240,008	304,015	344,052	444,005
Average	242,014	304,011	354,021	430,684

The results show that (Bảng 3.15) the thickness of the material layer increased due to the presence of TiO_2 and SnO_2. The PbO_2-TiO_2-SnO_2 composite has the greatest thickness (430,684 μm).

3.2.7. Determination of adhesion of electrode material layer

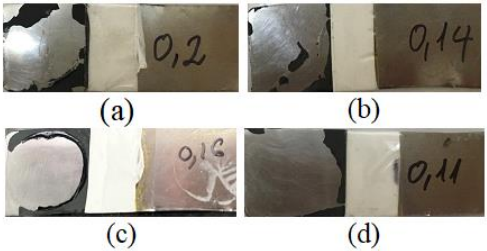

Figure 3.19. Adhesion of material layers on SS substrate (a) PbO_2, (b) PbO_2-TiO_2 composite (c) PbO_2-SnO_2 composite, (d) PbO_2-TiO_2-SnO_2 composite

The results showed that the adhesion of the PbO_2 layer on the SS was the highest (0.2 MPa) compared to that (0.11 MPa) of the PbO_2-TiO_2-SnO_2 composite. When TiO_2 and SnO_2 doped into the composite, they affected the adhesion of the material layer on the SS substrate (Figure 3.19b-d).

3.3. Study on electrochemical and photoelectrochemical properties of PbO_2 and its composite with TiO_2 and SnO_2

3.3.1. Cyclic voltammetry

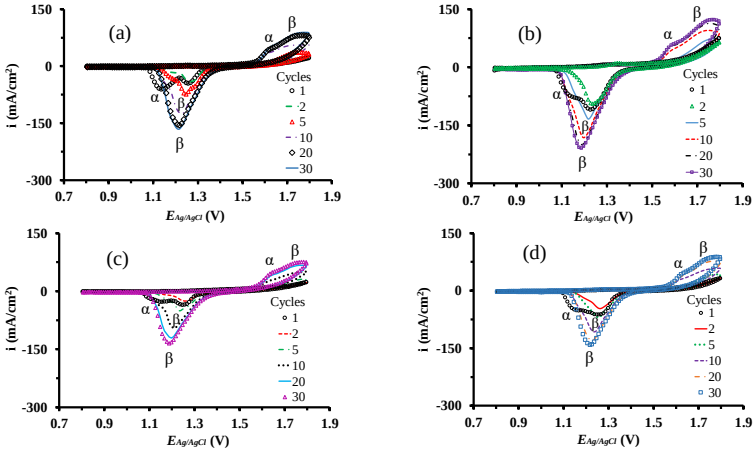

Figure 3.20. Cyclic voltammetry of electrodes (a) SS/PbO_2, (b) SS/PbO_2-TiO_2, (c) SS/PbO_2-SnO_2, (d) SS/PbO_2-TiO_2-SnO_2 (synthesis condition: 300 cycles, 50 mV/s) in 0.5 M H_2SO_4 with scan rate 100 mV/s

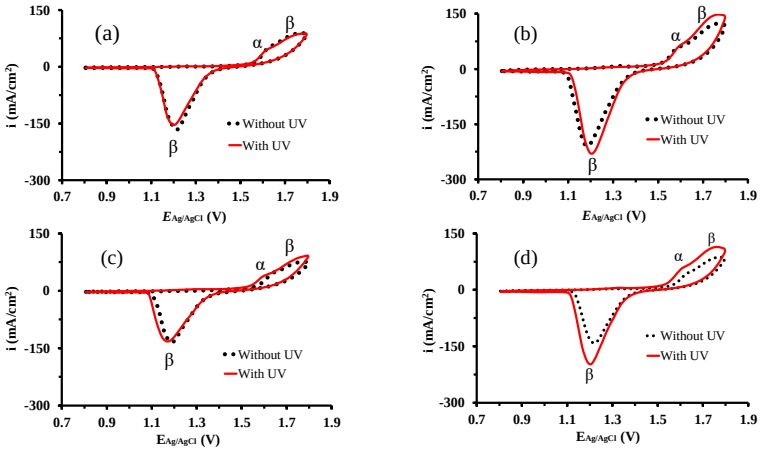

Figure 3.22. Cyclic voltammetry at the 30th cycle of electrodes (a) SS/PbO_2, (b) SS/ PbO_2-TiO_2, (c) SS/ PbO_2-SnO_2, (d) SS/PbO_2-TiO_2-SnO_2 in 0.5 M H_2SO_4 with and without UV

There are no oxidation peaks on the first cycle (Figure 3.20), but two reduction peaks can be clearly seen, characterizing a reduction of α and β-PbO_2 to $PbSO_4$. For the PbO_2 electrode, the two peaks α, β are clearly distinguished and the height of the α peak is larger than the β peak (figure 3.20a). However, for composites, the height of α peak is lower than that of β peak and the distinction between the two peaks is not clear (figure 3.20b-d), this is due to the influence of SnO_2 and TiO_2 in the composite.

The β-reduction peak in the second cycle decreased slightly compared to that in the first one, but then increased gradually with the number of scan cycles and was stabilized from the 20th cycle. However, the β-oxidation peak is slightly more visible from the fifth cycle, and both oxidation peaks belong to α and β-PbO_2 forms can be observed from the 10th cycle.

Under UV irradation, the oxidation peaks of the SS/PbO_2 electrode almost unchanged compared to that of the composite electrode increased sharply (Figure 3.22). This proves the photoelectrochemical activity of the composite electrode.

3.3.2. Determine the exchange current density

Under UV, the i_o value of electrodes increased, however, it of the SS/PbO_2 electrode increased less than that of the composite electrode. The SS/PbO_2-TiO_2-SnO_2 electrode has the highest i_o value in both with (151.5 μA/cm^2) and without (101.9 μA/cm^2) UV irradiation, indicating the best electrochemical activity (Table 3.20)

Table 3.20. Obtained i_o and E_o values of electrodes measured in 0.5 M H_2SO_4

Electrode	Without UV		With UV	
	i_o (μA/cm^2)	E_o (V)	i_o (μA/cm^2)	E_o (V)
SS/PbO_2	61.9	1.265	74.7	1.255
SS/PbO_2-TiO_2	53.4	1.254	79.3	1.256
SS/PbO_2-SnO_2	65.1	1.251	119.6	1.263
SS/PbO_2-TiO_2-SnO_2	101.9	1.220	151.5	1.219

3.3.3. Electrochemical impedance spectroscopy study

The results showed that the impedance spectrum of PbO_2 in 0.5 M H_2SO_4 under with and without UV light almost unchanged but it of the composites decreased sharply (Figure 3.27). This proves the photoelectrochemical activity of the composites.

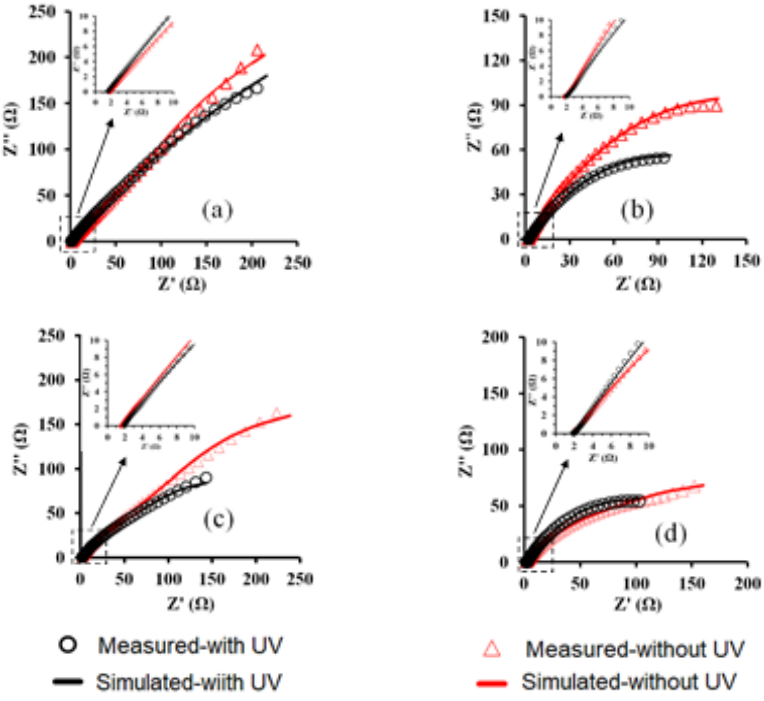

Figure 3.27. Nyquist diagrams of electrodes (a) SS/PbO_2, (b) SS/ PbO_2-TiO_2, (c) SS/ PbO_2-SnO_2, (d) SS/PbO_2-TiO_2-SnO_2 in 0.5 M H_2SO_4 with and without UV

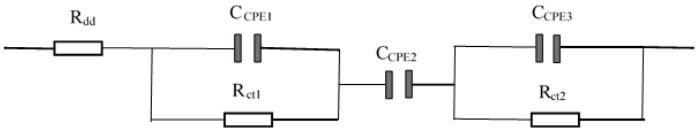

Figure 3.28. Electrical simulated circuits belong to Nyquist diagrams from Figure 3.27

R_{dd}: Solution resistance

Rc_{t1}: Charge transfer resistance of the processes occurring on the electrode surface

C_{CPE1}: Constant phase element of the electrode film

C_{CPE2}: Pseudo constant phase element

R_{ct2}: Charge transfer resistance of the processes occurring in the pore

C_{CPE3}: Constant phase element of the processes occurring in the pore

3.4. Study on factors affecting MO treatment on PbO_2 and composite PbO_2 with TiO_2; SnO_2 electrode

3.4.1. The effect of current density

When current density increased from 1.00 to 1.75 mA/cm^2, the treatment efficiency increased rapidly from 86.86% to 97.10%, corresponding to the remaining MO concentration in the solution also decreasing rapidly from 6.57 to 1.45 mg/L. However current density increased to 2.0 mA/cm^2, the treatment efficiency almost unchanged, reaching 97.17%. So current density of 1.75 mA/cm^2 was used for the following studies.

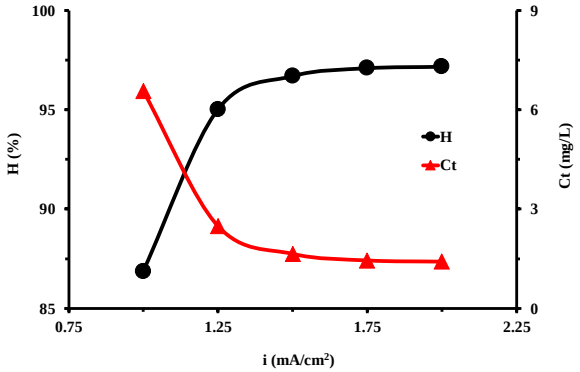

Figure 3.32. Colour removal efficiency and residual MO concentration after 50 min at different current density from MO concentration of 50 mg/L at pH 7

3.4.2. The effect of treatment time

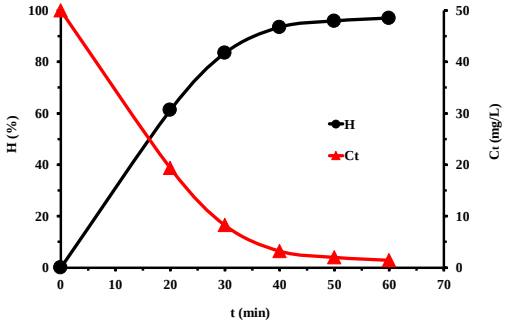

Figure 3.34. Colour removal efficiency and residual MO concentration after different treatment time from MO concentration of 50 mg/L at pH 7.

An increase in decolorization performance can be observed as the processing time is increased. However, the processing time increased from 50 to 60 min, the removal efficiency increased insignificantly at 97.15% and 97.55%, respectively. Therefore the optimal time for processing is 50 min.

3.4.3. The effect of initial concentration

When MO initial concentration was rased from 30 to 50 mg/L, the processing efficiency increased from 95.81 to 95.95% (the amount of MO that was treated as 28.74 and 47.98 mg/L, respectively). When MO initial concentration continuously increased, the treatment efficiency decreased. The optimal concentration is 50 mg/L with the efficiency of 97.15%.

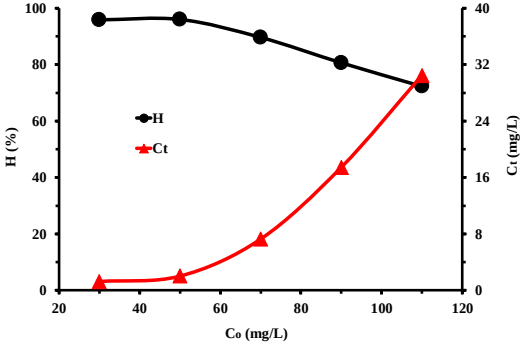

Figure 3.36. Colour removal efficiency and residual MO concentration after 50 min from different initial MO concentrations at pH 7.

3.4.4. The effect of solution pH

When the pH value increased, the treatment efficiency decreased and the the remaining MO concentration in the solution increased. With pH = 6, the treatment efficiency is 98.72% and this pH value is the most suitable.

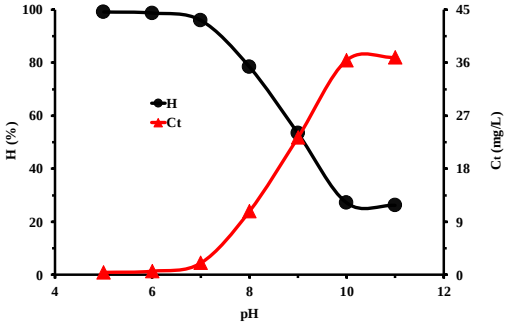

Figure 3.38. Colour removal efficiency and residual MO concentration after 50 min treatment at different pH from initial MO concentration of 50 mg/L.

3.4.5. Comparison of MO treatment efficiency under different treatment times at suitable conditions on fabricated electrodes

The MO removal efficiency on the SS/PbO_2-TiO_2-SnO_2 electrode was the highest (Figure 3.40) corresponding to residual MO concentration is the lowest (Figure 3.41). While the MO removal efficiency on the SS/PbO_2 electrode is the lowest corresponding to residual MO concentration is the largest.

At the treatment time of 10 minutes, the treatment efficiency and residual MO concentration on SS/PbO_2-TiO_2-SnO_2 composite electrode were 62.13% and 18.93 mg/L, respectively. While the MO removal efficiency and residual MO concentration on SS/PbO_2 electrode were 43.99% and 28 mg/L, respectively.

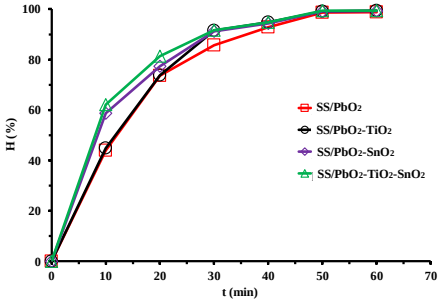

Figure 3.40. Colour removal efficiency on the electrodes after different treatment time at optimal condition (i = 1,75 mA/cm^2, C_o= 50 mg/L, pH=6)

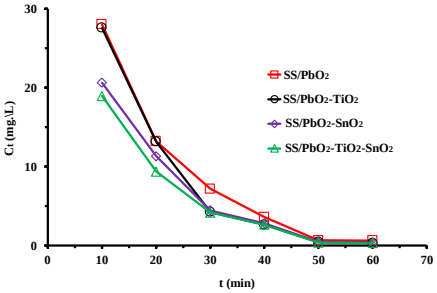

Figure 3.41. Residual MO concentration on the electrodes after different treatment time at optimal condition (i = 1,75 mA/cm^2, C_o= 50 mg/L, pH=6)

3.4.6. Comparison of MO removal efficiency on SS/PbO_2-TiO_2-SnO_2 composite electrodes under with and without UV.

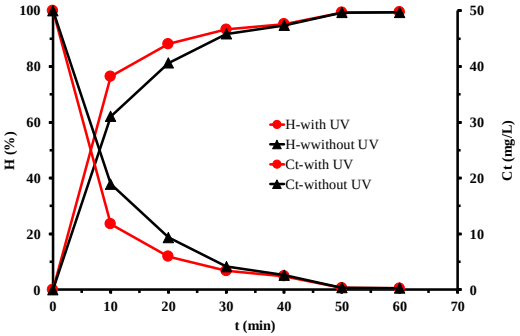

Figure 3.43. MO removal efficiency on the SS/PbO_2-TiO_2-SnO_2 composite electrode after different treatment time under with and without UV

Under UV irradiation, treatment efficiency rapidly increased in the early stages but removal efficiency unchanged in the end stages (Figure 3.43). At 10 minutes, the removal efficiency increased from 62.13% (without UV irradiation) to 76.45% (with UV irradiation) but at 60 minutes, the removal efficiency almost unchanged (99.45% and 99.51%, respectively). This proves that under UV light, the catalytic ability of the electrode increases thanks to improved i_o.

3.4.7. Study of MO elimination kinetics

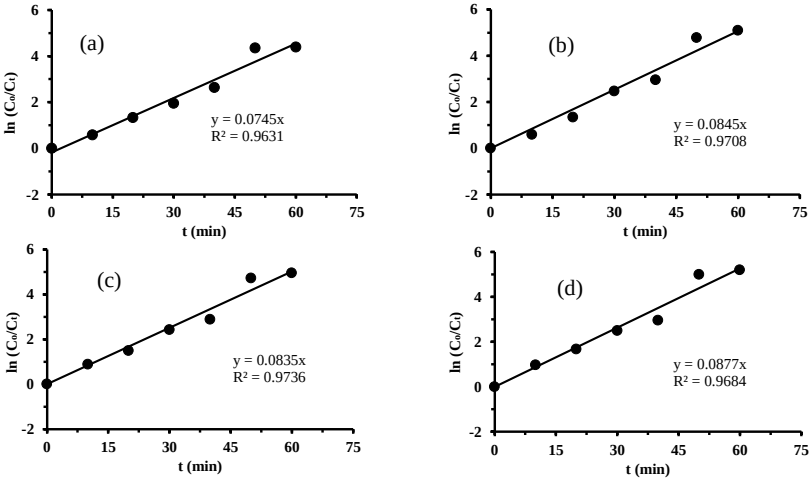

Figure 3.44. The diagram of ln (C_o/C_t) by treating time on the electrodes (a) SS/PbO_2; (b) SS/PbO_2-TiO_2; (c) SS/PbO_2-SnO_2; (d) SS/PbO_2-TiO_2-SnO_2 at optimal condition (i = 1,75 mA/cm^2, C_o= 50 mg/L, pH=6) without UV

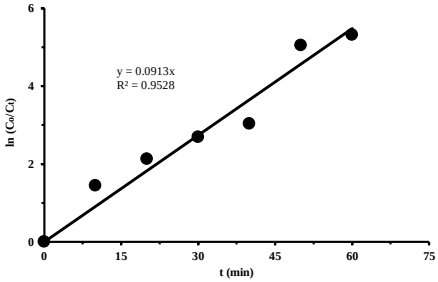

Figure 3.46. The diagram of ln (C_o/C_t) by treating time on SS/PbO_2-TiO_2-SnO_2 electrode under UV irradiation (i = 1,75 mA/cm^2, C_o= 50 mg/L, pH=6)

From the diagram of ln (C_o/C_t) according to treating time (figure 3.44 and 3.46) we can determine the reaction rate constant k and the R^2 value. The results showed that the linearity is relatively high from 0.9528 to 0.9736, so the kinetic of the MO oxidation reaction followed the pseudo-first order.

3.4.8. Investigation of the ORP

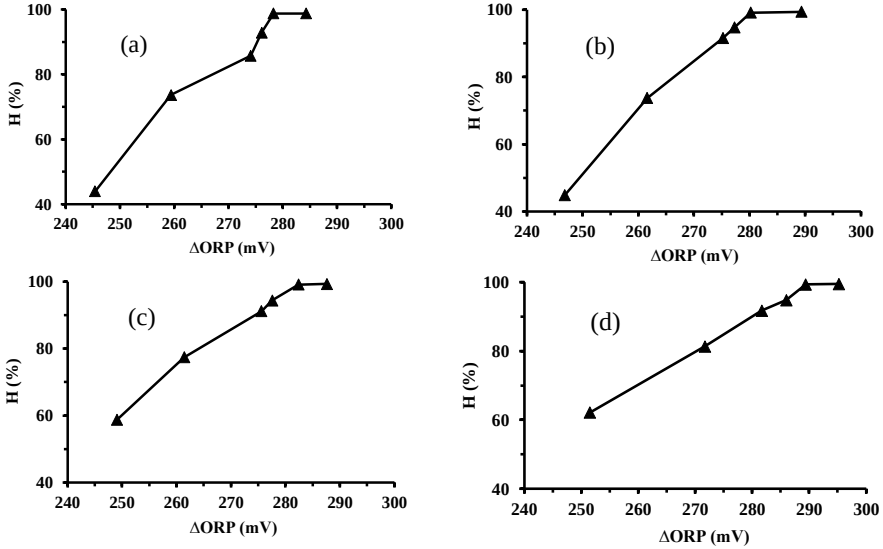

Figure 3.47. The diagram of removal efficiency by ORP on the electrodes a) SS/PbO_2; (b) SS/PbO_2-TiO_2; (c) SS/PbO_2-SnO_2; (d) SS/PbO_2-TiO_2-SnO_2 at optimal condition (i = 1,75 mA/c^2, C_o= 50 mg/L, pH=6) without UV

As we know ORP is considered for indicating the level of MO solution treatment. The value of ORP can describe the quality of the solution, while the

ΔORP between the inlet and outlet wastewater reflects the pollutant removal efficiency. The higher the ORP value is, the better the oxidation state of the solution is. The higher the ΔORP value is, the higher the pollutant removal efficiency is. Figure 3.47 shows the MO removal efficiency on different electrodes according to ΔORP. Observing the figure, when the ΔORP value increases, the treatment efficiency also increases, that is, the higher the oxidation state of the solution and the cleaner the solution.

From figure 3.48, under UV irradiation, the treatment efficiency increases and the ΔORP index increases compared to that without UV irradiation. This proves the photocatalytic activity of the SS/PbO_2-TiO_2-SnO_2 composite electrode.

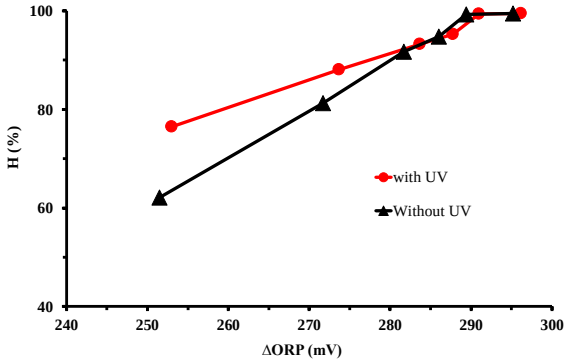

Figure 3.48. The graph of MO treatment efficiency by ΔORP on SS/PbO_2-TiO_2-SnO_2 composite electrode at optimal condition (i = 1,75 mA/cm^2, C_o= 50 mg/L, pH = 6) with and without UV

3.4.9. Proposing a MO treatment mechanism

The MO processing reaction mechanism can occur in two steps as follows:

Initially the hydroxyl radicals (˙OH) are formed by the oxidation of water according to the reaction (3.10). They are physically adsorbed on the anode surface (AS) and become very active able to oxidize organic compounds to reactive intermediates (3.11).

$$AS + H_2O \rightarrow AS(^{\cdot}OH) + H^+ + e^- \quad (3.10)$$

$$AS(^{\cdot}OH) + MO \rightarrow AS + \text{intermediates} \quad (3.11)$$

Then MO will be attacked by hydroxyl radicals (·OH) at the electron-rich site such as -N=N- to decompose into phenolic compounds. These compounds are oxidized to quinones, organic carboxylic acids and end products (CO_2 and H_2O) as the reaction (3.12).

$$AS(\cdot OH) + \text{intermediates} \rightarrow AS + CO_2 + H_2O + \text{inorganic ions} \quad (3.12)$$

From figure 3.49 shows that with the processing time of 10 minutes (Figure 3.49b) on the spectrum, there are many characteristic peaks of different fragments. After 50 minutes of processing (Figure 3.49c) the number of peaks appears is very little and the height of the characteristic peaks is greatly reduced. This proves that before forming CO_2 and H_2O, MO is oxidized to intermediate compounds and after 50 minutes of treatment, almost all substances in the solution have been removed. Based on this result, we can propose a MO processing mechanism as shown in Figure 3.50.

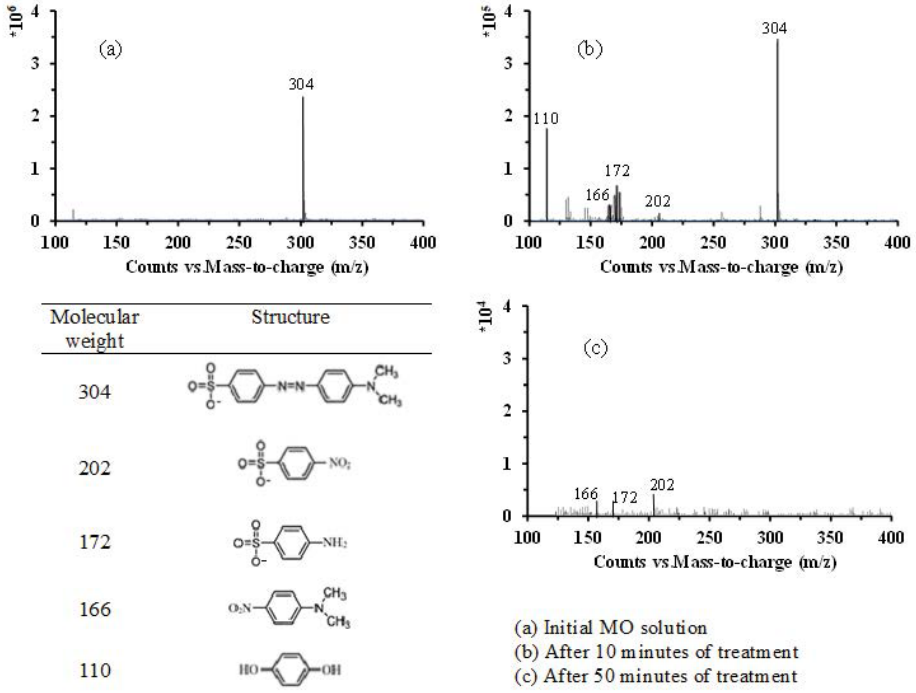

Figure 3.49. HPLC/MS chromatographs before and after degradation of MO

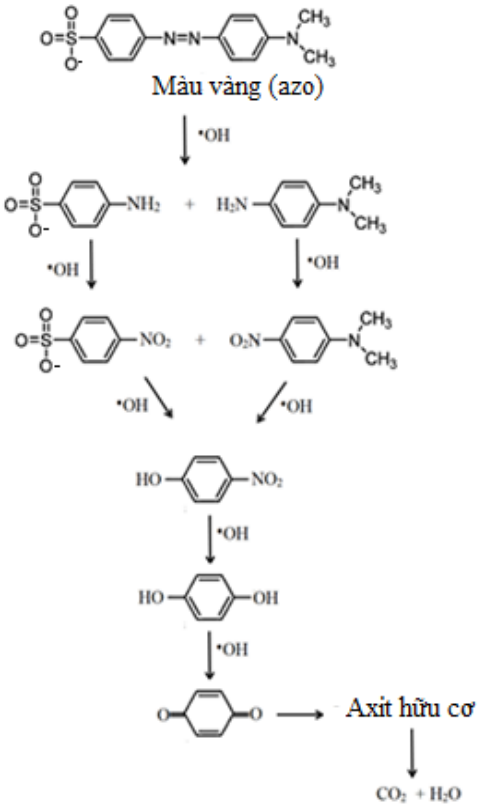

Figure 3.50. MO treatment mechanism

To confirm the presence of ·OH group during MO treatment, the thesis used tert-butanol as quenching agent for ·OH group. The graph of the relationship between MO and ΔORP removal efficiency over treatment time with and without tert-butanol is shown in Figure 3.51. The results shown that at the same treatment time, in the presence of tert-butanol, both the treatment efficiency and the ΔORP value decreased. Because some of the newly formed ·OH groups reacted with tert-butanol (reaction (3.13)), so the ability to oxidize MO in solution was reduced. Thus, it proves that the MO processing mechanism proposed above is completely suitable.

$$\cdot OH + (CH_3)_3COH \rightarrow H_2O + \cdot CH_2C(CH_3)_2OH \qquad (3.13)$$

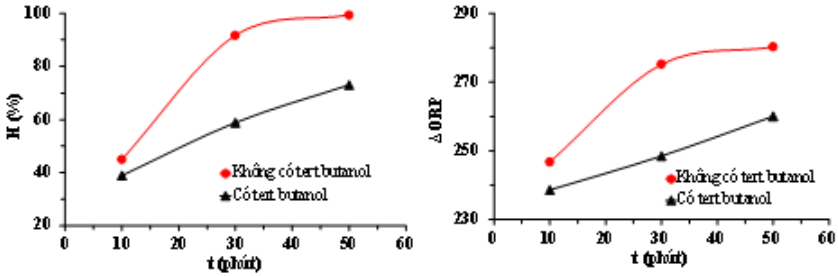

Figure 3.51. MO removal efficiency and ORP value by treating time with and without tert-butanol

CONCLUSIONS

1. Successfully synthesized SS/PbO_2 and (SS/PbO_2-TiO_2, SS/PbO_2-SnO_2, SS/PbO_2-TiO_2-SnO_2) electrodes by CV method. At optimal synthesis conditions (scanning speed 50 mV/s, 300 cycles, 2.0 g/L TiO_2, 1.5 g/L SnO_2) SS/PbO_2-TiO_2-SnO_2 electrode has the best electrocatalytic activity.

2. By CV and X-ray diffraction method, the existence of two α, β allotropic forms in PbO_2 and composites based on PbO_2, TiO_2, SnO_2 have been demonstrated. The presence of TiO_2, SnO_2 has been demonstrated in composite materials by EDX, Element-mapping and SEM methods.

3. Under UV irradiation, the SS/PbO_2-TiO_2, SS/PbO_2-SnO_2, SS/PbO_2-TiO_2-SnO_2 composite electrodes anodic current density (CV spectrum), exchange current density (I-E polarization curve) increased and the total electrochemical impedance (EIS spectrum) decreased. This proves that the composites have photoelectrochemical activity.

4. Suitable MO treatment conditions have been determined (i = 1.75 mA/cm^2, C_o = 50 mg/L, t = 50 min, pH = 6). MO processing efficiency on composite electrodes reached from 99.11 to 99.32%, a slight increase compared to that on SS/PbO_2 electrode (98.72%), in which MO treatment efficiency reached the highest on SS /PbO_2-TiO_2-SnO_2 (99.32%). The MO removal efficiency depends on the oxidation–reduction index (ΔORP), the higher this index reflects the higher the treatment efficiency and the cleaner the solution.

5. The kinetics of MO processing was determined according to the pseudo-first order with a good linearity (0.9528-0.9736) on both SS/PbO_2 and composite electrodes with and without UV irradiation.

6. A two-stage MO treatment mechanism has been proposed: First, the SS/PbO_2 and composites electrodes will oxidize water to create $^{\cdot}OH$ groups. Then the $^{\cdot}OH$ groups will oxidize MO to form intermediate organic compounds and finally to CO_2 and H_2O according to the reactions ((3.10)-(3.12)).

THE NEW FINDING OF THE DOCTORAL THESIS

- Successfully synthesized two-component (SS/PbO_2-TiO_2; SS/PbO_2-SnO_2) and three-component composite electrodes (SS/PbO_2-TiO_2-SnO_2) by CV method. Composite materials achieve nanostructure.
- It has been demonstrated that composite electrodes with photoelectrochemical activity are arranged in order:

$$SS/PbO_2\text{-}TiO_2 < SS/PbO_2\text{-}SnO_2 < SS/PbO_2\text{-}TiO_2\text{-}SnO_2.$$

- Proven SS/PbO_2-TiO_2; SS/PbO_2-SnO_2 and SS/PbO_2-TiO_2-SnO_2 composite electrode could be to catalyze electrochemical and photoelectrochemical for Methyl Ogrange processing, in which the Methyl Ogrange processing efficiency of the three-component composite electrode is the highest (99.36%) under UV light for 50 minutes.
- Studying the kinetics of MO processing, proving that the efficiency of Methyl Ogrange processing depends on the ΔORP index.

LIST OF PUBLICATIONS

1. **Phạm Thị Tốt**, Mai Thị Thanh Thùy, Nguyễn Thế Duyến, Phan Thị Bình, "Tổng hợp và nghiên cứu tính chất của PbO_2 trên nền thép không gỉ", Tạp chí Khoa học, Trường Đại học Sư phạm Hà Nội 2, **2020**, 69, 27-34.
2. **Tot T.Pham**, Thuy T. T. Mai, and Binh T. Phan, "Removal of methyl orange from aqueous solution by electrochemical process using stainless steel/PbO_2-TiO_2 stable electrode", Desalination and Water Treatment, **2022**, 66, 202-211 **(SCIE)**
3. **Pham Thi Tot**, Mai Thi Thanh Thuy, Phan Thi Binh, "Electrochemical characterization of PbO_2-TiO_2 composite prepared on stainless steel substrate by cyclic voltammetrry method", Vietnam Journal of Science and Technology**, 2022**, 60 (4), 631-640.
4. **Phạm Thị Tốt**, Mai Thị Thanh Thùy, Phan Thị Bình, "Nghiên cứu xử lý metyl da cam bằng phương pháp oxi hóa điện hóa trên điện cực SS/PbO_2" Hội nghị khoa học toàn quốc về Dệt may - Da giầy, lần thứ 3 - NSCTEX2022, **2022**, 36-41.